Journal of Mathematical Modeling
Vol. 10, No. 3, 2022. pp. 387-405. Research Article

JMM

Numerical solution of one-dimensional Sine-Gordon equation using rational radial basis functions

Mansour Shiralizadeh[†*], Amjad Alipanah[†], Maryam Mohammadi[‡]

[†]*Department of Applied Mathematics, University of Kurdistan, Sanandaj, Iran*
[‡]*Faculty of Mathematical Sciences and Computer, Kharazmi University, Tehran, Iran*
Email(s): m.shiralizadeh@uok.ac.ir, a.alipanah@uok.ac.ir, m.mohammadi@khu.ac.ir

Abstract. In this paper, we use the rational radial basis function (RRBF) method for solving the one dimensional Sine-Gordon (SG) equation, especially the case with steep front or sharp gradient solutions. The time and spatial derivatives are approximated by the finite difference and RRBF method, respectively. Some numerical experiments are given in both perturbed and unperturbed cases, and are compared with some other numerical methods to confirm the good accuracy of the presented method. The conservation law of energy is also investigated.

Keywords: Sine-Gordon equation, Radial basis function, Rational radial basis function method, Conservation law.
AMS Subject Classification 2010: 65N99, 65N35, 74G15, 97N40.

1 Introduction

In this paper, we consider the Sine-Gordon equation as follows

$$\frac{\partial^2 u}{\partial t^2} - \frac{\partial^2 u}{\partial x^2} + \sin u = \varepsilon_1 \frac{\partial u}{\partial t} + \varepsilon_2 u + \varepsilon_3 \sin 2u, \quad a \le x \le b, \ t \ge 0, \tag{1}$$

with the initial conditions

$$u(x,0) = f(x), \quad u_t(x,0) = g(x), \tag{2}$$

and Dirichlet or Neumann boundary conditions as

$$u(a,t) = h_1(t), \quad u(b,t) = h_2(t), \tag{3}$$

or

$$u_x(a,t) = k_1(t), \quad u_x(b,t) = k_2(t), \tag{4}$$

*Corresponding author.
Received: 28 August 2021 / Revised: 30 November 2021 / Accepted: 12 December 2021
DOI: 10.22124/jmm.2021.20458.1780

where $\varepsilon_j, j = 1,2,3$ is a constant and ε_1 is the damping coefficient [23]. Equation (1) corresponds to the unperturbed SG equation for $\varepsilon_j = 0, j = 1,2,3$.

The SG equation is a ubiquitous physical model that describes nonlinear oscillations in various settings, such as the propagation of fluxion in Josephson junctions, the motion of a rigid pendular, dislocation in metals, solid state physics, nonlinear optics, and interaction of atomic chains [22].

Since the analytical solution of the SG equation exists only in particular conditions, and the presence of small perturbations may lead to equations that are difficult to integrate exactly, this equation must be studied numerically. The SG equation has been solved using many numerical methods such as thin plate splines RBF method [4], finite difference method [20], boundary integral equation method [3], modified cubic B-spline collocation method [18], multiquadric quasi-interpolation method [9], barycentric rational interpolation and local RBF method [10], spectral element method [17], differential quadrature method [14], Chebyshev tau meshless method [26], finite elements method [1], and pseudospectral method [27].

It is well-known that the solution of unperturbed SG equation has a conserved quantity, namely the energy, given as follows [3, 7]:

$$E(t) = \int_a^b \left(u_x^2 + u_t^2 + 2(1-\cos u)\right) dx.$$

Despite traditional numerical methods for solving partial differential equations (PDEs), meshless methods need no mesh generation (see e.g [6, 11–13, 16, 19, 21]). Among meshless methods, radial basis function (RBF) methods are simple enough to allow modelling rather high dimensional problems [6, 24, 28].

The main problem is that the RBF methods may produce oscillatory solutions when the underlying solutions have steep gradients or discontinuities. In such situations, the rational radial basis function (RRBF) method is capable of giving more accurate solutions away from the steep fronts and discontinuities [25]. In 2009, Jakobsson et al. presented a RRBF method to interpolate functions with steep gradients [8]. Sarra and Bai [25] used RRBF method to solve PDEs in which the solutions have steep gradients and discontinuities. In [5] De Marchi et al. presented RRBF-based partition of unity interpolation.

In this paper, we use the RRBF method to obtain the numerical solution of (1) with the conditions given in the Eqs. (2)-(4). The time and spatial derivatives are approximated by the finite difference and RRBF methods, respectively. We also analyze the effects of different perturbations, damping, amplification and perturbations on the SG equation when the initial conditions correspond to the exact solutions of the unperturbed equation [15].

This paper is organized as follows. A concise introduction of the RBF and RRBF methods is given in Section 2. In Section 3, implementation of the method is given. We analyze stability issues in Section 4. The numerical results are presented in Section 5. Section 6 is also devoted to a brief conclusion.

2 RBF and Rational RBF interpolation

2.1 RBF interpolation

Let $\Omega \subseteq \mathbb{R}^d$ be a bounded set, $X = \{\boldsymbol{x}_1^c, \ldots, \boldsymbol{x}_N^c\} \subseteq \Omega$ be a set of N distinct center points, and $\mathbf{f} = \{f(\boldsymbol{x}_1^c), \ldots, f(\boldsymbol{x}_N^c)\}$ be a set of function values. The RBF

$$\phi(\boldsymbol{x}) = \phi\left(\|\boldsymbol{x} - \boldsymbol{x}^c\|_2, \varepsilon\right), \quad \boldsymbol{x}, \boldsymbol{x}^c \in \mathbb{R}^d$$

is a function of one variable $r = \|\boldsymbol{x} - \boldsymbol{x}^c\|_2$ that is centered at $\boldsymbol{x}^c$, where ε is a free parameter known as the shape parameter [6]. In Table 1 we list some commonly used infinitely smooth RBFs. In this work

Table 1: Some global RBFs.

Name of RBF	Abbreviation	$\phi(r),\ r \geq 0$
Multiquadric	MQ	$\sqrt{1+(\varepsilon r)^2}$
Inverse multiquadric	IMQ	$\frac{1}{\sqrt{1+(\varepsilon r)^2}}$
Inverse quadratic	IQ	$\frac{1}{1+(\varepsilon r)^2}$
Generalizaed multiquadric	GMQ	$(1+(\varepsilon r)^2)^{\beta}$
Gaussian	GA	$e^{-(\varepsilon r)^2}$

we use $d = 1$ and work with the Inverse quadratic which is a strictly positive definite RBF. The RBF interpolant takes the form

$$s(\boldsymbol{x}) = \sum_{j=1}^{N} a_j \, \phi\left(\|\boldsymbol{x} - \boldsymbol{x}_j^c\|_2, \varepsilon\right), \tag{5}$$

where the coefficients a_j are obtained by solving the linear system $B\mathbf{a} = \mathbf{f}$, based on the interpolation conditions $s(\boldsymbol{x}_i^c) = f_i$, where $\mathbf{f} = [f(\boldsymbol{x}_1^c), \ldots, f(\boldsymbol{x}_N^c)]^T$. The entries of the matrix B are of the form

$$b_{ij} = \phi\left(\|\boldsymbol{x}_i^c - \boldsymbol{x}_j^c\|_2, \varepsilon\right), \quad i, j = 1, \ldots, N.$$

The matrix B is a symmetric positive definite matrix and so invertible. The values of the interpolant (5) at M points $\boldsymbol{x}_i$ are computed by $H.\mathbf{a}$, where the entries of the evaluation matrix H are of the form

$$h_{ij} = \phi\left(\|\boldsymbol{x}_i - \boldsymbol{x}_j^c\|_2, \varepsilon\right), \quad i = 1, \ldots, M, \ \ j = 1, 2, \ldots, N. \tag{6}$$

The first derivative of the RBF interpolant is of the form

$$D(s(\boldsymbol{x})) = \sum_{j=1}^{N} a_j \, D\left(\phi\left(\|\boldsymbol{x} - \boldsymbol{x}_j^c\|_2, \varepsilon\right)\right),$$

thus

$$D(s(\boldsymbol{x}_i^c)) = \sum_{j=1}^{N} a_j \, D\phi\left(\|\boldsymbol{x}_i^c - \boldsymbol{x}_j^c\|_2, \varepsilon\right),$$

i.e. $D\mathbf{f} \simeq H_D\mathbf{a}$, where the entries of H_D are of the form

$$(H_D)_{ij} = D\phi\left(\|\boldsymbol{x}_i^c - \boldsymbol{x}_j^c\|_2, \varepsilon\right), \quad i, j = 1, \ldots, N.$$

The second derivative of the RBF interpolant is of the form

$$D(D(s(\boldsymbol{x}))) = \sum_{j=1}^{N} a_j \, D\left(D\phi\left(\|\boldsymbol{x} - \boldsymbol{x}_j^c\|_2, \varepsilon\right)\right),$$

thus

$$D(D(s(\boldsymbol{x}_i^c))) = \sum_{j=1}^{N} a_j \, D\left(D\phi\left(\|\boldsymbol{x}_i^c - \boldsymbol{x}_j^c\|_2 \, , \varepsilon\right)\right),$$

i.e., $D(D\mathbf{f}) \simeq H_{DD}\mathbf{a}$, where the entries of H_{DD} are of the form

$$(H_{DD})_{ij} = D\left(D\phi\left(\|\boldsymbol{x}_i^c - \boldsymbol{x}_j^c\|_2 \, , \varepsilon\right)\right), \quad i,j = 1,\ldots,N.$$

In the following theorem we give an error bound [6].

Theorem 1. *Suppose that $\phi \in C(\Omega \times \Omega)$ is a strictly positive definite RBF, the points $X = \{\boldsymbol{x}_1^c,\ldots,\boldsymbol{x}_N^c\} \subseteq \Omega$ are distinct, and s is the interpolant to $f \in \mathscr{N}_\phi(\Omega)$. Then for all $\boldsymbol{x} \in \Omega$ we have*

$$|f(\boldsymbol{x}) - s(\boldsymbol{x})| \leq P_{\phi,X}(\boldsymbol{x})\|f\|_{\mathscr{N}_{\phi(\Omega)}},$$

where $\mathscr{N}_\phi(\Omega)$ is the native reproducing kernel Hilbert space corresponding to the symmetric positive definite RBF.

2.2 Rational RBF interpolation

The standard RBF interpolant has problems such as ill-conditioning, particularly when the shape parameter approaches to zero and these problems might lead to inaccurate solutions, especially for the functions with steep front or sharp gradients. So the RRBF interpolant arises [8].

The RRBF interpolant of function f is of the form

$$\mathscr{R}(\boldsymbol{x}) = \frac{p(\boldsymbol{x})}{q(\boldsymbol{x})},$$

which satisfies in the interpolation conditions $\mathscr{R}(\boldsymbol{x}_k^c) = f(\boldsymbol{x}_k^c)$, $k = 1,2,\ldots,N$, and $p(\boldsymbol{x})$ and $q(\boldsymbol{x})$ are the RBF interpolants

$$p(\boldsymbol{x}) = \sum_{j=1}^{N} a_j^p \, \phi\left(\|\boldsymbol{x} - \boldsymbol{x}_j^c\|_2 \, , \varepsilon\right),$$

and

$$q(\boldsymbol{x}) = \sum_{j=1}^{N} a_j^q \, \phi\left(\|\boldsymbol{x} - \boldsymbol{x}_j^c\|_2 \, , \varepsilon\right).$$

Let $\mathbf{p} = [p(\boldsymbol{x}_1^c),\ldots,p(\boldsymbol{x}_N^c)]^T$ and $\mathbf{q} = [q(\boldsymbol{x}_1^c),\ldots,q(\boldsymbol{x}_N^c)]^T$. It is easy to see that imposing the interpolation conditions leads to an undetermined system of equations which needs an extra condition in order to be uniquely solved [8, 25]. This causes the native space semi-norms of the RBF interpolants $p(\boldsymbol{x})$ and $q(\boldsymbol{x})$ are minimized which in turn leads to a minimization problem with the solution $\mathbf{q}$ that is the eigenvector corresponding to the smallest eigenvalue problem $S\mathbf{q} = \lambda\mathbf{q}$, where

$$S = \operatorname{diag}\left(1/\left(\frac{\mathbf{f}^2}{\|\mathbf{f}\|_2^2} + 1\right)\right)\left(\frac{DB^{-1}D}{\|\mathbf{f}\|_2^2} + B^{-1}\right),$$

and $D = \mathrm{diag}\,(f(\boldsymbol{x}_1^c),\ldots,f(\boldsymbol{x}_N^c))$. Moreover, $\mathbf{f}^2$ represents an elementwise squaring of the elements of the vector $\mathbf{f}$ and division is elementwise. After $\mathbf{q}$ is found, the vector $\mathbf{p}$ is obtained by $\mathbf{p} = D\mathbf{q}$. So the expansion coefficients of the RBF interpolants are found by solving the following linear systems

$$Ba^p = \mathbf{p}, \quad \text{and} \quad Ba^q = \mathbf{q}. \tag{7}$$

Now the rational interpolant at M points $\boldsymbol{x}_i$ is evaluated by

$$\mathbf{R} = \frac{Ha^p}{Ha^q}, \tag{8}$$

where $\mathbf{R} = [\mathscr{R}(\boldsymbol{x}_1),\ldots,\mathscr{R}(\boldsymbol{x}_M)]^T$, H is the RBF evaluation matrix (6), and division is elementwise.

The first and second derivatives of the rational interpolant at N centers $\boldsymbol{x}_i^c$ can be obtained by applying quotient rule as below

$$\begin{aligned}
\mathbf{R}_1^{'} &= \frac{(Ba^q).(H_D a^p) - (Ba^p).(H_D a^q)}{(Ba^q)^2}, \\
\mathbf{R}_1^{''} &= \frac{2(Ba^p).(H_D a^q)^2 + (Ba^q)^2.(H_{DD} a^p)}{(Ba^q)^3} - \frac{(Ba^q).\Big(2\,(H_D a^p).(H_D a^q) + (Ba^p).(H_{DD} a^q)\Big)}{(Ba^q)^3},
\end{aligned} \tag{9}$$

where $\mathbf{R}_1^{'} = \left[\mathscr{R}^{'}(\boldsymbol{x}_1^c),\ldots,\mathscr{R}^{'}(\boldsymbol{x}_N^c)\right]^T$, $\mathbf{R}_1^{''} = \left[\mathscr{R}^{''}(\boldsymbol{x}_1^c),\ldots,\mathscr{R}^{''}(\boldsymbol{x}_N^c)\right]^T$.

From equations (7) and (8) we conclude that the RRBF interpolant is constructed by means of the standard RBF interpolation matrix B. Suppose that $\mathbf{p}$ and $\mathbf{q}$ are the values obtained by sampling some functions v and w in $\mathscr{N}_\phi(\Omega)$, respectively. Then the following error estimate is given for the RRBF interpolation [5].

Proposition 1. *Suppose that $\phi \in C(\Omega\times\Omega)$ is a strictly positive definite RBF, the points $X = \{\boldsymbol{x}_1^c,\ldots,\boldsymbol{x}_N^c\} \subseteq \Omega$ are distinct, and $\mathscr{R}$ is the RRBF interpolant to $f \in \mathscr{N}_\phi(\Omega)$. Then for all $\boldsymbol{x} \in \Omega$ we have*

$$|f(\boldsymbol{x}) - \mathscr{R}(\boldsymbol{x})| \le \frac{1}{|q(\boldsymbol{x})|}\left(|f(\boldsymbol{x})|\|w\|_{\mathscr{N}_\phi(\Omega)} + \|v\|_{\mathscr{N}_\phi(\Omega)}\right) P_{\phi,X}(\boldsymbol{x}).$$

3 A numerical scheme for solving SG equation using RRBF

In this section, we develop RRBF to study the unperturbed and perturbed SG equation subject to Dirichlet or Neumann boundary conditions. By discretizing the SG equation

$$\frac{\partial^2 u}{\partial t^2} - \frac{\partial^2 u}{\partial x^2} + \sin u = \varepsilon_1 \frac{\partial u}{\partial t} + \varepsilon_2 u + \varepsilon_3 \sin 2u,$$

in time, we get

$$\begin{aligned}
\frac{\mathbf{U}(x,t+\Delta t) - 2\mathbf{U}(x,t) + \mathbf{U}(x,t-\Delta t)}{(\Delta t)^2} &= \mathbf{U}_{xx}(x,t) - \sin(\mathbf{U}(x,t)) \\
+ \varepsilon_1 \frac{\mathbf{U}(x,t+\Delta t) - \mathbf{U}(x,t-\Delta t)}{2\Delta t} &+ \varepsilon_2 \mathbf{U}(x,t) + \varepsilon_3 \sin(2\mathbf{U}(x,t)),
\end{aligned}$$

where Δt is the time step size. Now let $a = x_1^c < x_2^c < \ldots < x_{N-1}^c < x_N^c = b$, and

$$\mathbf{U}^n = \left[U\left(x_1^c,\cdot\right),\ldots,U\left(x_N^c,\cdot\right)\right]^T, \quad \mathbf{U}_{xx}^n = \left[U_{xx}\left(x_1^c,t\right),\ldots,U_{xx}\left(x_N^c,t\right)\right]^T.$$

Then

$$\begin{aligned}\mathbf{U}^{n+1} = \tfrac{2}{2-\varepsilon_1\Delta t}\Bigg(&\left(2+\varepsilon_2(\Delta t)^2\right)\mathbf{U}^n - (1+\tfrac{\varepsilon_1}{2}\Delta t)\mathbf{U}^{n-1}\\ &+(\Delta t)^2(\mathbf{U}_{xx})^n - (\Delta t)^2\sin(\mathbf{U}^n) + \varepsilon_3(\Delta t)^2\sin(2\mathbf{U}^n)\Bigg).\end{aligned} \tag{10}$$

According to (10), initial values $\mathbf{U}^0$, $\mathbf{U}^{-1}$ and $(\mathbf{U}_{xx})^0$ are required in order to obtain $\mathbf{U}^1$. Using the initial conditions (2), we get $\mathbf{U}^0 = \mathbf{f}$ and $\mathbf{U}_{xx}^0 = \mathbf{f}''$, where $\mathbf{f} = [f(x_1^c),\ldots,f(x_N^c)]^T$ and $\mathbf{f}'' = \left[f''(x_1^c),\ldots,f''(x_N^c)\right]^T$. The second initial condition also gives

$$\frac{\mathbf{U}(x,t_1) - \mathbf{U}(x,t_{-1})}{2\Delta t} = \mathbf{g}(x),$$

so $\mathbf{U}^{-1} = \mathbf{U}^1 - 2\Delta t\mathbf{g}(x)$, where $\mathbf{g}(x) = [g(x_1^c),\ldots,g(x_N^c)]^T$. Therefore, Eq. (10) results

$$\begin{aligned}\mathbf{U}^1 = \tfrac{1}{2}\Big(&\left(2+\varepsilon_2\left(\Delta t\right)^2\right)\mathbf{f}(x) + 2\Delta t\left(1+\tfrac{\varepsilon_1}{2}\Delta t\right)\mathbf{g}(x)\Big)\\ &+\tfrac{1}{2}\Big(\left(\Delta t\right)^2\mathbf{f}''(x) - \left(\Delta t\right)^2\sin\left(\mathbf{f}(x)\right) + \varepsilon_3\left(\Delta t\right)^2\sin\left(2\mathbf{f}(x)\right)\Big).\end{aligned} \tag{11}$$

In order to obtain $\mathbf{U}^{n+1}$ for $n \geq 1$ in the iterative relation (10), the values $\mathbf{U}^n$, $\mathbf{U}^{n-1}$ and $(\mathbf{U}_{xx})^n$ are required where $\mathbf{U}^n$ and $\mathbf{U}^{n-1}$ are known and the only unknown is $(\mathbf{U}_{xx})^n$ which is given by computing (9) when $\mathbf{U}^n$ is considered instead of $\mathbf{f}$.

Lemma 1. *(Local truncation error). Assume that u be the exact solution of the SG equation (1) and at least $u \in C^3$ (with respect to the time). If e^n is truncation error in semi-discrete problem (10), then $|e^n| = O((\Delta t)^2)$.*

Proof. Let

$$\begin{aligned}e^n = &\frac{u\left(x,t_n+\Delta t\right) - 2u\left(x,t_n\right) + u\left(x,t_n-\Delta t\right)}{\left(\Delta t\right)^2} - u_{xx}\left(x,t_n\right) + \sin\left(u\left(x,t_n\right)\right)\\ &- \varepsilon_1\frac{u\left(x,t_n+\Delta t\right) - u\left(x,t_n-\Delta t\right)}{2\Delta t} - \varepsilon_2 u(x,t_n) - \varepsilon_3\sin\left(2U(x,t_n)\right).\end{aligned} \tag{12}$$

Then using Taylor's theorem we have

$$u\left(x,t_n+\Delta t\right) = u^n + \Delta t(\frac{\partial u}{\partial t})^n + \frac{(\Delta t)^2}{2!}(\frac{\partial^2 u}{\partial t^2})^n + \frac{(\Delta t)^3}{3!}(\frac{\partial^3 u}{\partial t^3})^n + \frac{(\Delta t)^4}{4!}(\frac{\partial^4 u}{\partial t^4})^n + \cdots, \tag{13}$$

and

$$u\left(x,t_n-\Delta t\right) = u^n - \Delta t(\frac{\partial u}{\partial t})^n + \frac{(\Delta t)^2}{2!}(\frac{\partial^2 u}{\partial t^2})^n - \frac{(\Delta t)^3}{3!}(\frac{\partial^3 u}{\partial t^3})^n + \frac{(\Delta t)^4}{4!}(\frac{\partial^4 u}{\partial t^4})^n + \cdots. \tag{14}$$

After substituting (13) and (14) in (12), we have

$$e^n = (\frac{\partial^2 u}{\partial t^2})^n - u_{xx}^n + sin(u^n) - \varepsilon_1(\frac{\partial u}{\partial t})^n - \varepsilon_2 u^n$$
$$-\varepsilon_3 \sin(2u^n) + (\Delta t)^2 \left(\frac{1}{12}(\frac{\partial^4 u}{\partial t^4})^n - \frac{1}{6}\varepsilon_1(\frac{\partial^3 u}{\partial t^3})^n + \cdots \right).$$

Hence $|e^n| = O((\Delta t)^2)$. □

3.1 Implementation of boundary conditions

3.1.1 Dirichlet boundary conditions

In order to implement Dirichlet boundary conditions (3) in (10), we directly replace $U(\boldsymbol{x}_1^c, t_{n+1})$ and $U(\boldsymbol{x}_N^c, t_{n+1})$ with $h_1(t_{n+1})$ and $h_2(t_{n+1})$, respectively.

3.1.2 Neumann boundary conditions

Since the values of the function u are required in (10), we use the following forward and backward difference formulas for implementing Neumann boundary conditions (4)

$$\frac{u(\boldsymbol{x}_2^c, t) - u(a,t)}{\delta_1} = k_1(t), \quad \text{and} \quad \frac{u(b,t) - u(\boldsymbol{x}_{N-1}^c, t)}{\delta_2} = k_2(t).$$

where $\delta_1 = \boldsymbol{x}_2^c - a$, and $\delta_2 = b - \boldsymbol{x}_{N-1}^c$. Therefore

$$u(a,t) = u(\boldsymbol{x}_2^c, t) - \delta_1 k_1(t), \quad \text{and} \quad u(b,t) = u(\boldsymbol{x}_{N-1}^c, t) + \delta_2 k_2(t).$$

So we replace $U(\boldsymbol{x}_1^c, t_{n+1})$ with $u(a, t_{n+1})$ and $U(\boldsymbol{x}_N^c, t_{n+1})$ with $u(b, t_{n+1})$ in (10).

Now we summarize the RRBF method for solving the SG equation in the following algorithm written in the MATLAB notation.

Algorithm.

1. Choose N centers from the domain set $[a,b]$.
2. Choose the parameters Δt, ε (shape parameter), and ε_1, ε_2, ε_3 in (1).
3. Set $B = \left(\phi \left(\|\boldsymbol{x}_i^c - \boldsymbol{x}_j^c\|, \varepsilon \right) \right)_{1 \le i,j \le N}$ based on the centers.
4. Set

$$H_D = \left(D\phi \left(\|\boldsymbol{x}_i^c - \boldsymbol{x}_j^c\|, \varepsilon \right) \right)_{1 \le i,j \le N},$$
$$H_{DD} = \left(D\left(D\phi \left(\|\boldsymbol{x}_i^c - \boldsymbol{x}_j^c\|, \varepsilon \right) \right) \right)_{1 \le i,j \le N}.$$

5. Obtain Cholesky decomposition of the matrix B and set $L = \text{chol}(B, \text{'lower'})$.
6. Use the decomposition to calculate the inverse of B as $Bi = L' \setminus (L \setminus \text{eye}(N))$.

7. Calculate the initial solution $\mathbf{U}^0$ from (2) then use (11) to calculate $\mathbf{U}^1$.
8. The approximate solution $\mathbf{U}^{n+1}$ at successive time levels is obtained from (10) and steps 9-14.
9. Set $D = \text{diag}(\mathbf{U}^n)$.
10. Set $S = \text{diag}(1./(K*(\mathbf{U}^n).\hat{}2+1))*(K*D*Bi*D+Bi)$ where $K = 1./\text{sum}((\mathbf{U}^n).\hat{}2)$.
11. Find the eigenvector $\mathbf{q}$ corresponding to the smallest eigenvalue of the matrix S by $\mathbf{q} = \text{eigs}(S,1,0)$.
12. Set $\mathbf{p} = D*\mathbf{q}$.
13. Solve $Ba^p = \mathbf{p}$ and $Ba^q = \mathbf{q}$ as $a^p = L^{'}\backslash(L\backslash\mathbf{p})$ and $a^q = L^{'}\backslash(L\backslash\mathbf{q})$.
14. Set

$$(\mathbf{U}_{xx})^n = \frac{2(Ba^p).(H_D a^q)^2 + (Ba^q)^2.(H_{DD}a^p)}{(Ba^q)^3}$$

$$-\frac{(Ba^q).(2(H_D a^p).(H_D a^q) + (Ba^p).(H_{DD}a^q))}{(Ba^q)^3}.$$

4 Stability issue

Since the RRBF interpolant is constructed by using the standard RBF interpolation matrix, the RRBF method can also suffer from instability issues, especially when $\varepsilon \to 0$. In fact, serious problems of ill-conditioning may occur by choosing wrong values of the shape parameter, particularly for infinitely smooth RBFs. According to the Uncertainty Principle, the shape parameter ε must not be too small for well-conditioning reason, but for better accuracy of the RBF interpolation, small shape parameters are required. Actually the more favorably valued quantity is the less favorably valued the other is. So we choose the shape parameter ε by using the pseudocode given in [24] so that the collocation matrix B has a condition number, $\kappa(B)$, in the range $10^{13} \le \kappa(B) \le 10^{15}$.

5 Numerical results

In this section, we consider five and three examples for the unperturbed and perturbed SG equation, respectively, in order to confirm the accuracy and efficiency of the method. We use L_∞, L_2 and RMS error norms as follows

$$L_\infty = \|\mathbf{U}-\mathbf{u}\|_\infty, \quad L_2 = \|\mathbf{U}-\mathbf{u}\|_2, \quad RMS = \sqrt{\tfrac{1}{N}\|\mathbf{U}-\mathbf{u}\|_2},$$

where $\mathbf{U}$, $\mathbf{u}$ are the numerical and the exact solutions, respectively. Moreover, the following uniformly spaced centers

$$x_j^c = a + \frac{j-1}{N-1}(b-a), \quad j = 1,2,\ldots,N,$$

or non-uniformly spaced centers

$$x_j = \frac{1}{2}\left(-(b-a)\left(\frac{\arcsin(0.999\cos((j-1)\pi/(N-1)))}{\arcsin(0.999)}\right)+(b+a)\right), \tag{15}$$

which are clustered mildly around the boundaries [25], are used. The energy is also evaluated using the composite trapezoidal rule for integration.

Example 1. Consider the unperturbed SG equation (1) in $-20 \leq x \leq 20$ with the initial conditions [3]

$$u(x,0) = 4\arctan\left(\exp\left(\frac{x}{\sqrt{1-c^2}}\right)\right),$$
$$u_t(x,0) = \frac{-2c\cdot\operatorname{sech}\left(\frac{x}{\sqrt{1-c^2}}\right)}{\sqrt{1-c^2}}.$$

The analytical solution is given as

$$u(x,t) = 4\arctan\left(\exp\left(\frac{x-c\cdot t}{\sqrt{1-c^2}}\right)\right).$$

The Dirichlet boundary conditions are derived from the analytical solution. The results are obtained using $c = 0.5$, $\Delta t = 0.01$, $\varepsilon = 2$, and $N = 500$ uniformly spaced centers. The L_∞, L_2, RMS errors and energy are reported in Table 2. It can be noted from Table 2 that the results are in good agreement with those reported in [3] and the conservation of energy is also confirmed.

Table 2: Invariants and errors of Example 1.

t	L_∞	L_2	*RMS*	Energy
0.25	1.1894e-04	2.4100e-04	1.0778e-05	18.4383
0.5	1.2227e-04	3.4300e-04	1.5339e-05	18.4383
0.75	1.2225e-04	4.1281e-04	1.8461e-05	18.4383
1	1.2046e-04	4.6189e-04	2.0657e-05	18.4383
2	1.1437e-04	5.1809e-04	2.3170e-05	18.4383
5	1.3423e-04	4.3038e-04	1.9247e-05	18.4383
10	1.7801e-04	5.1966e-04	2.3240e-05	18.4383
15	2.3543e-04	6.5199e-04	2.9158e-05	18.4383
20	3.1339e-04	8.4070e-04	3.7579e-05	18.4383

Example 2. In this example, we examine the unperturbed SG equation (1) in $-20 \leq x \leq 20$ with the initial conditions [22]

$$u(x,0) = 4\arctan\left(\exp\left(\frac{-x}{\sqrt{1-c^2}}\right)\right), \quad c = 0.95,$$

$$u_t(x,0) = \frac{2c\cdot\operatorname{sech}\left(\frac{x}{\sqrt{1-c^2}}\right)}{\sqrt{1-c^2}}.$$

The exact solution is given as

$$u(x,t) = 4\arctan\left(\exp\left(-\frac{x-c\cdot t}{\sqrt{1-c^2}}\right)\right).$$

We extract the Dirichlet boundary conditions from the exact solution and use shape parameter $\varepsilon = 2$, $\Delta t = 0.01$ and $N = 500$ uniformly spaced centers. We advance the solution in time up to $t = 20$, when the steep front approaches to the end of the domain. The graphs of the exact and approximate solutions

and their first and second derivatives as well as the pointwise error distribution of the solutions at the times $t = 2$ and $t = 10$ are shown in Figure 1. It is seen that the error reaches it maximum value when the steep front arises and this can be advanced when time goes on. In Table 3, we reported the L_∞, L_2, RMS errors, and energy at several times. It should be pointed that the method is accurate and the energy is conservative.

Table 3: Invariants and errors of Example 2.

t	L_∞	L_2	RMS	Energy
0.25	1.3086e-04	3.9330e-04	1.7589e-05	51.1403
0.5	1.4274e-04	4.9815e-04	2.2278e-05	51.1403
0.75	1.9470e-04	5.9493e-04	2.6606e-05	51.1403
1	2.5476e-04	7.0399e-04	3.1483e-05	51.1403
2	5.1335e-04	1.2000e-03	5.1525e-05	51.1403
5	1.4000e-03	3.2000e-03	1.4163e-04	51.1403
10	2.6000e-03	7.4000e-03	3.3026e-04	51.1403
20	4.9000e-03	1.2000e-03	5.3738e-04	51.0421

Example 3. Consider the unperturbed SG equation (1) in $-10 \leq x \leq 10$ with the initial conditions

$$\begin{aligned} &u(x,0) = 0, \\ &u_t(x,0) = 4\mathrm{sech}(x), \end{aligned}$$

and the exact solution [3]

$$u(x,t) = 4\arctan(\mathrm{sech}(x)t).$$

We derive the Dirichlet boundary conditions from the exact solution and use $N = 401$ uniformly spaced centers, and a shape parameter $\varepsilon = 3$. The numerical results at different times up to $t = 20$ with $\Delta t = 0.01$ are shown in Table 4. It is evident that the energy is conserved as time advances and the better accuracy is obtained compared with [3]. The graphs of the pointwise error distribution, approximate and exact solutions for $t = 5$ and $t = 15$ are given in Figure 2. Although the error becomes larger around the point $x = 0$ at the time $t = 5$, it tends to be better at the time $t = 15$. This is due to fact that the solution becomes smoother near the point $x = 0$, as time advances.

Example 4. Consider the unperturbed SG equation (1) in $-20 \leq x \leq 20$ with the initial conditions

$$\begin{aligned} &u(x,0) = 4\arctan\left(c\sinh\left(\tfrac{x}{\sqrt{1-c^2}}\right)\right), \\ &u_t(x,0) = 0. \end{aligned}$$

The Neumann boundary conditions are driven from the following exact solution [2]

$$u(x,t) = 4\arctan\left(\frac{c\sinh\left(\frac{x}{\sqrt{1-c^2}}\right)}{\cosh\left(\frac{ct}{\sqrt{1-c^2}}\right)}\right).$$

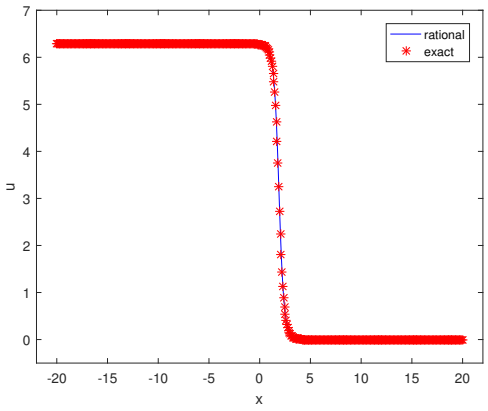

(a) RRBF and exact solutions at $t = 2$.

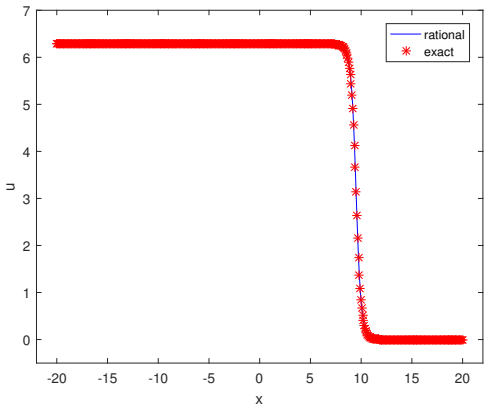

(b) RRBF and exact solution at $t = 10$.

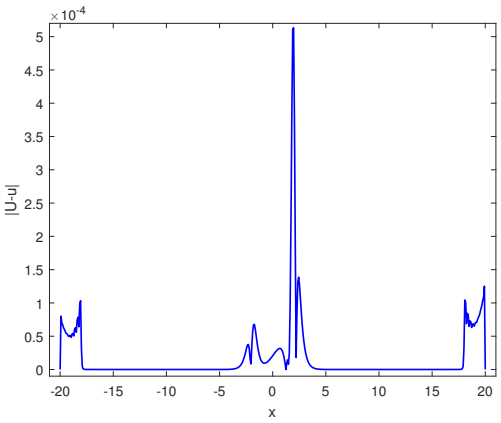

(c) Pointwise error at $t = 2$.

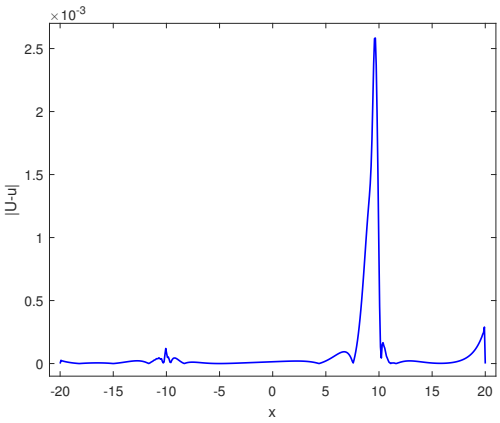

(d) Pointwise error at $t = 10$.

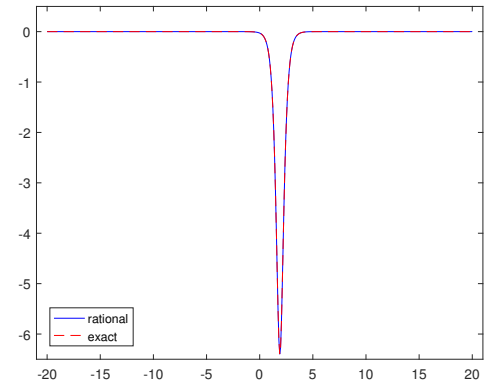

(e) Approximate and exact first derivative at $t = 2$.

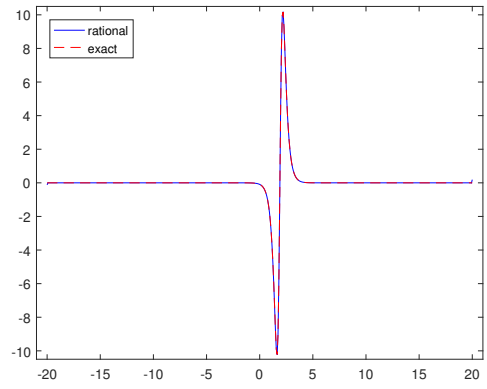

(f) Approximate and exact second derivative at $t = 2$.

Figure 1: Numerical results of Example 2.

Table 4: Invariants and errors of Example 3.

	RRBF				[3]	
N	L_∞	L_2	*RMS*	Energy	L_∞	Energy
0.25	3.0169e-05	1.4400e-04	7.1908e-06	32.0125	-	-
0.5	4.6806e-05	2.4339e-04	1.2154e-05	32.0458	-	-
0.75	5.1706e-05	3.0422e-04	1.5192e-05	32.0314	-	-
1	5.2994e-05	3.5484e-04	1.7720e-05	32.0033	1.678e-04	31.9950
2	7.8976e-05	6.7163e-04	3.3540e-05	31.9409	4.237e-04	31.9935
5	3.2159e-04	3.000e-03	1.4923e-04	31.9223	3.257e-04	31.9942
10	1.4000e-03	1.2600e-02	6.2974e-04	31.9210	4.829e-03	31.9948
15	3.2000e-03	2.8900e-02	1.4000e-03	31.9209	1.124e-02	31.9949
20	5.8000e-03	5.1700e-02	2.6000e-03	31.9208	1.155e-02	31.9949

Table 5 shows the numerical results for $c = 0.5$, $\Delta t = 0.01$, $\varepsilon = 1.5$, and $N = 500$ non-uniform set of center points given by (15). The pointwise error distribution, and the exact and approximate solutions for $t = 10$ are plotted in Figure 3.

Table 5: Errors of Example 4.

	RRBF			[2]
N	L_∞	L_2	*RMS*	L_∞
0.25	1.7063e-07	7.7252e-07	3.4548e-08	-
0.5	6.2197e-07	2.8680e-07	1.2826e-07	-
0.75	1.2060e-06	5.7380e-06	2.5661e-07	-
1	1.7856e-06	8.7756e-06	3.9246e-07	-
2	3.5867e-06	1.8297e-05	8.1828e-07	1.2760e-04
10	9.8879e-06	6.3119e-05	2.8227e-06	1.9115e-04

Example 5. Consider the unperturbed SG equation (1) in $-20 \leq x \leq 20$ with the initial conditions

$$\begin{aligned} u(x,0) &= 0, \\ u_t(x,0) &= \frac{4}{\sqrt{1+c^2}\cosh\left(\frac{x}{\sqrt{1+c^2}}\right)}. \end{aligned}$$

The Neumann boundary conditions are driven from the analytical solution [26]

$$u(x,t) = 4\arctan\left(\frac{1}{c}\sin\left(\frac{ct}{\sqrt{1+c^2}}\right)\operatorname{sech}\left(\frac{x}{\sqrt{1+c^2}}\right)\right).$$

Table 6 shows the numerical results for $c = 0.5$, $\Delta t = 0.01$, $\varepsilon = 1.5$, and $N = 400$ non-uniform set of center points given by (15). The pointwise error distribution, and the exact and approximate solutions for $t = 10$ are plotted in Figure 4.

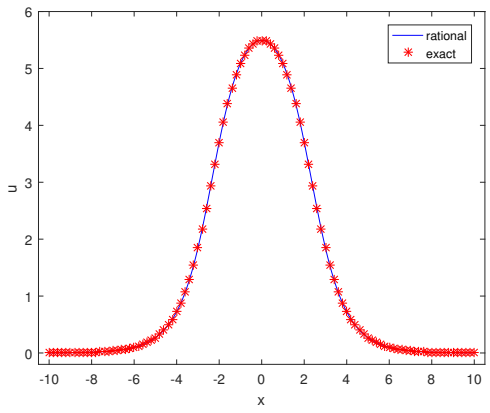

(a) RRBF and exact solutions at $t = 5$.

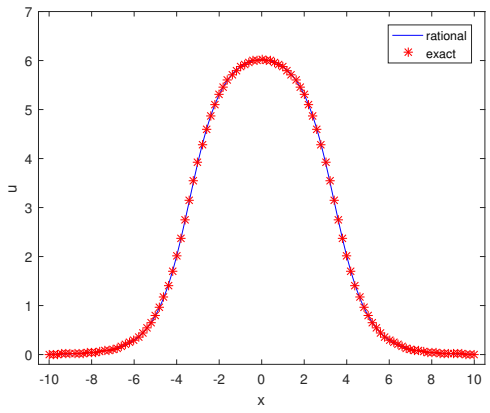

(b) RRBF and exact solution at $t = 15$.

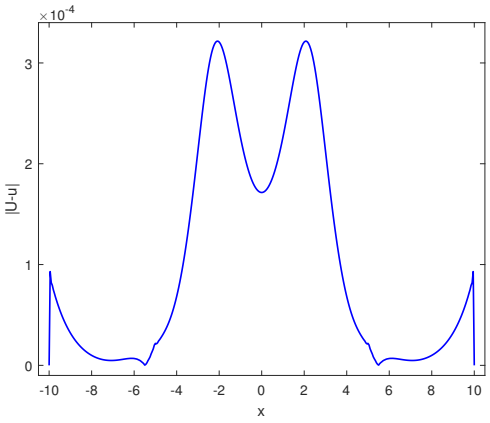

(c) Pointwise error at $t = 5$.

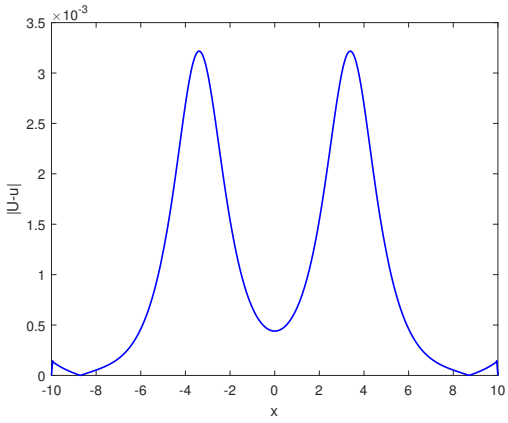

(d) Pointwise error at $t = 15$.

Figure 2: Numerical results of Example 3.

Example 6. In this example, we consider the following perturbed SG equation in the domain $0 \leq x \leq 2$ [26],

$$u_{tt} + u_t = u_{xx} - 2\sin(u) + \pi^2 \exp(-t)\sin(\pi x) + 2\sin(\exp(-t)\sin(\pi x)),$$

with the initial conditions

$$u(x,0) = \sin(\pi x),$$
$$u_t(x,0) = -\sin(\pi x).$$

The exact solution is also given as $u(x,t) = \exp(-t)\sin(\pi x)$, where the Dirichlet boundary conditions are extracted from it. Table 7 shows the numerical results for $\varepsilon = 4$, $\Delta t = 0.0001$, and $N = 100$ non-uniform set of center points given by (15). The pointwise error distribution, and the exact and approximate solutions for $t = 3$ are plotted in Figure 5.

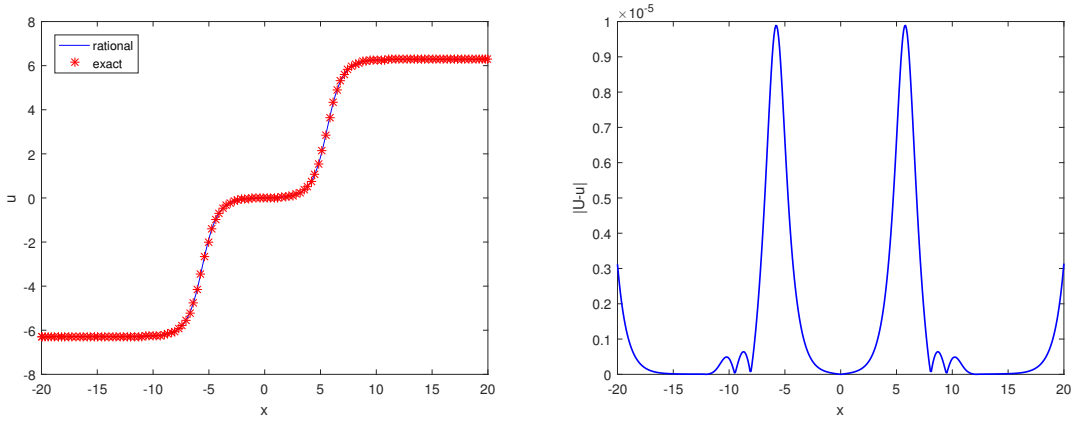

(a) RRBF and exact solutions at $t = 10$.

(b) Pointwise error at $t = 10$.

Figure 3: Numerical results of Example 4.

Table 6: Errors of Example 5.

t	L_∞	L_2	RMS
0.25	2.4605e-05	8.8287e-05	4.4144e-06
0.5	3.9633e-05	1.5091e-04	7.5457e-06
0.75	4.5464e-05	1.8809e-04	9.4043e-06
1	4.7695e-05	2.1464e-04	1.0732e-05
2	7.4064e-05	3.8999e-04	1.9499e-05
5	4.9787e-04	3.1000e-03	1.5720e-04
10	3.4972e-05	2.0864e-04	1.0423e-05
15	2.2000e-03	1.2700e-02	6.3470e-04
20	3.1000e-03	1.7900e-02	8.9460e-04

Example 7. In this example, we use the RRBF method to numerically solve the following perturbed one-dimensional SG equation [23]

$$u_{tt} - u_{xx} + \sin(u) = \varepsilon_3 \sin(2u),$$

in the region $-25 \leq x \leq 75$ with the shape parameter $\varepsilon = 0.75$, $\Delta t = 0.01$, $c = 0.3$, $\varepsilon_3 = 0.05$, and $N = 801$ uniformly spaced centers. The numerical solutions for $t \in [0,2]$ with the initial and Dirichlet boundary conditions corresponding to the following exact solutions of the unperturbed SG equation

$$u(x,t) = 4\arctan\left(\frac{\sqrt{1-c^2}\sin(ct)}{c\cosh(\sqrt{1-c^2}x)}\right), \qquad u(x,t) = 4\arctan\left(\exp\left(\frac{x-ct}{\sqrt{1-c^2}}\right)\right),$$

are shown in Figures 6 and 7, respectively. They are in agreement with the results obtained by [23].

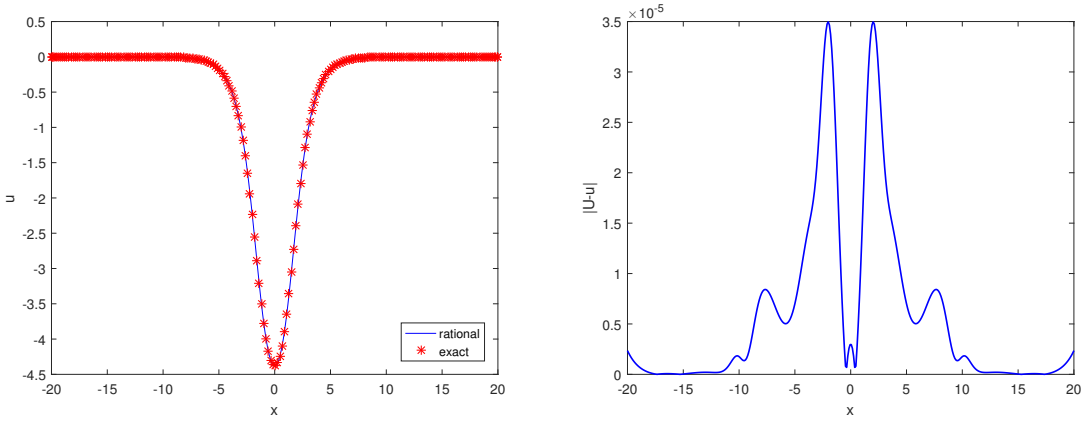

(a) RRBF and exact solutions at $t = 10$.

(b) Pointwise error at $t = 10$.

Figure 4: Numerical results of Example 5.

Table 7: Errors of Example 6.

t	L_∞	L_2	RMS
0.25	1.2415e-08	4.7771e-08	4.7771e-09
0.5	9.7852e-09	5.0558e-08	5.0558e-09
0.75	1.0054e-08	4.5503e-08	4.5503e-09
1	9.1300e-09	4.3728e-08	4.3728e-09
2	3.0602e-08	8.9129e-08	8.9129e-09
3	6.8361e-08	2.9280e-07	2.9280e-08
4	5.5599e-08	2.8004e-07	2.8004e-08
5	1.8905e-08	9.6526e-08	9.6526e-09

Example 8. In this example, the numerical solution of the following perturbed one-dimensional SG equation [23]

$$u_{tt} - u_{xx} + \sin(u) = \varepsilon_1 u_t + \varepsilon_2 u,$$

in the region $-25 \leq x \leq 75$ with the shape parameter $\varepsilon = 0.75$, $\Delta t = 0.01$, $c = 0.3$, $\varepsilon_1 = 0.01$, $\varepsilon_2 = 0.01$ and $N = 801$ uniformly spaced centers is investigated. The numerical solutions for $t \in [0,2]$ with the initial and Dirichlet boundary conditions corresponding to the following exact solutions of the unperturbed SG equation

$$u(x,t) = 4\arctan\left(\frac{c\sinh\frac{x}{\sqrt{1-c^2}}}{\cosh\frac{ct}{\sqrt{1-c^2}}}\right), \qquad u(x,t) = 4\arctan\left(\frac{\sinh\frac{ct}{\sqrt{1-c^2}}}{c\cosh\frac{x}{\sqrt{1-c^2}}}\right),$$

are shown in Figures 8 and 9, respectively. They are in agreement with the results obtained by [23].

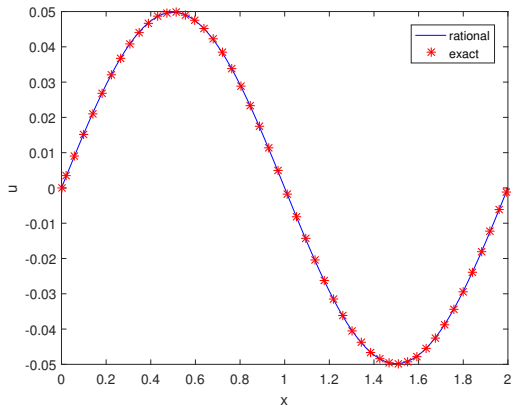

(a) RRBF and exact solutions at $t = 3$.

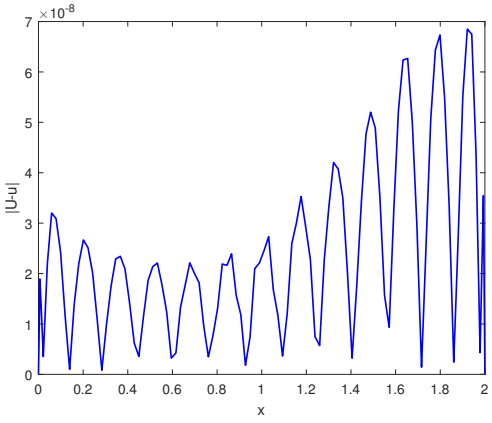

(b) Pointwise error at $t = 3$.

Figure 5: Numerical results of Example 6.

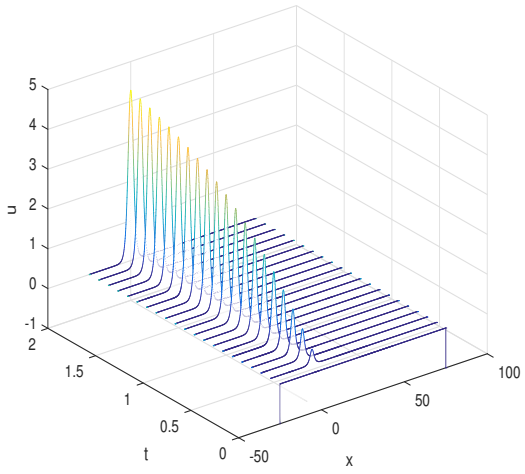

Figure 6: Numerical solution of Example 7.

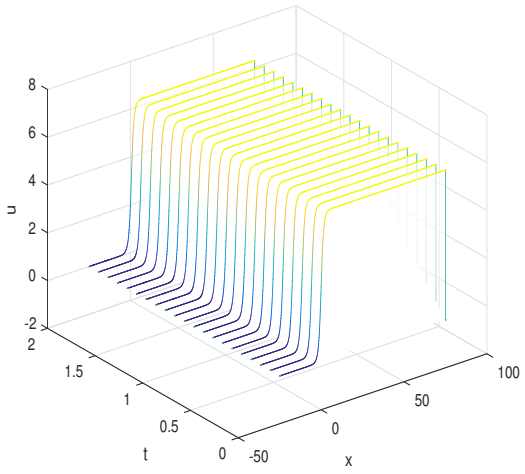

Figure 7: Numerical solution of Example 7.

6 Conclusion

In this paper we use the rational radial basis function (RRBF) method to numerically solve the perturbed and unperturbed SG equation with Dirichlet or Neumann boundary conditions, especially in cases that the solution is a function with steep front or sharp gradients. The time and spatial derivatives are approximated by the finite difference and RRBF method, respectively. Numerical results show that our method is of satisfactory accuracy, preserves the conservation law of energy, and behaves more accurate compared to the methods available in the literature. This technique can be used to solve several time-dependent PDEs such as Black-Scholes, Korteweg de Vries (KdV), Allen-Cahn that we left for future works.

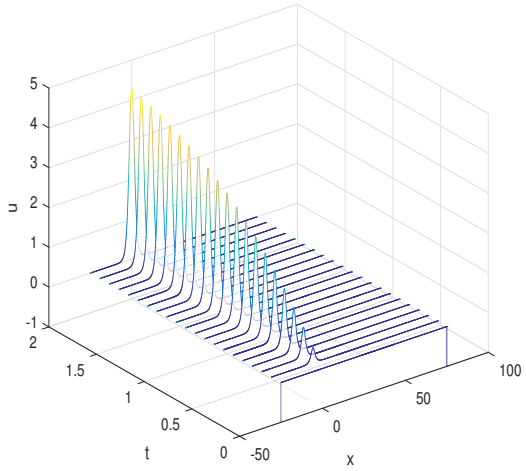

Figure 8: Numerical solution of Example 8.

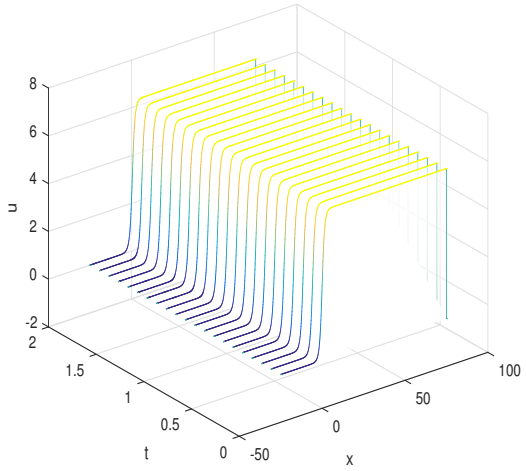

Figure 9: Numerical solution of Example 8.

References

[1] J. Argyris, M. Hasse, J.C. Heinrich, *Finite element approximation to two-dimensional Sine-Gordon solutions*, Comput. Methods Appl. Mech. Engrg. **86** (1991) 1-26.

[2] A.G. Bratsos, *A fourth order numerical scheme for the one-dimensional sine-Gordon equation*, Int. J. Comput. Math. **85** (2008) 1083-1095.

[3] M. Dehghan, D. Mirzaei, *The boundary integral equation approach for numerical solution of the one-dimensional Sine-Gordon equation*, Numer. Methods Partial Differ. Equ. **24** (2008) 1405-1415.

[4] M. Dehghan, A. Shokri, *A numerical method for one-dimensional nonlinear Sine-Gordon equation using collocation and radial basis functions*, Numer. Methods Partial Differ. Equ. **24** (2008) 687-698.

[5] S. De Marchi, A. Martinez, E. Perracchione, *Fast and stable rational RBF-based partition of unity interpolation*, J. Comput. Appl. Math. **349** (2019) 331-343.

[6] G.E. Fasshauer, *Meshfree Approximation Methods with* MATLAB, World Scientific, 2007.

[7] B.Y. Guo, P.J. Pascual, M.J. Rodriguez, L. Vazquez, *Numerical solution of the Sine-Gordon equation*, Appl. Math. Comput. **18** (1986) 1-14.

[8] S. Jakobsson, B. Andersson, F. Edelvik, *Rational radial basis function interpolation with applications to antenna design*, J. Comput. Appl. Math. **233** (2009) 889-904.

[9] Z.-W. Jiang, R.-H. Wang, *Numerical solution of one-dimensional Sine-Gordon equation using high accuracy multiquadric quasi-interpolation*, Appl. Math. Comput. **218** (2012) 7711-7716.

[10] R. Jiwari, *Barycentric rational interpolation and local radial basis functions based numerical algorithms for multidimensional sine-Gordon equation*, Numer. Methods Partial Differential Equations **37** (3) (2020) 1965-1992.

[11] R. Jiwari, A. Gerisch, *A local radial basis function differential quadrature semidiscretisation technique for the simulation of time-dependent reaction-diffusion problems*, Eng. Comput. **38** (2021) 2666-2691.

[12] R. Jiwari, S. Kumar, R.C. Mittal, *Meshfree algorithms based on radial basis functions for numerical simulation and to capture shocks behavior of Burgers' types problems*, Eng. Comput. **36** (2019) 1142-1168.

[13] R. Jiwari, S. Kumar, R.C. Mittal, J. Awrejcewicz, *A meshfree approach for analysis and computational modeling of non-linear Schrdinger equation*, Comp. Appl. Math. **39** (2020) 1-25.

[14] R. Jiwari, S. Pandit, R.C. Mittal, *Numerical simulation of two-dimensional sine-Gordon solitons by differential quadrature method*, Comput. Phys. Comm. **183** (2012) 600-616.

[15] Y.S. Kivshar, B.A. Malomed, *Many-particle effects in nearly integrable systems*, Phys. D **24** (1987) 125-154.

[16] S. Kumar, R. Jiwari, R.C. Mittal, *Numerical simulation for computational modelling of reaction-diffusion Brusselator model arising in chemical processes*, J. Math. Chem. **57** (2019) 149-179.

[17] M. Lotfi, A. Alipanah, *Legendre spectral element method for solving Sine-Gordon equation*, Adv. Differ. Equ. **113** (2019) 1-15.

[18] R.C. Mittal, R. Bhaita, *Numerical solution of nonlinear Sine-Gordon equation by modified cubic B-Spline collocation method*, Int. J. Partial. Differ. Equ. **2014** (2014) 1-8.

[19] M. Mohammadi, R. Mokhtari, R. Schaback, *A meshless method for solving the 2D Brusselator reaction-diffusion system*, Comput. Model. Eng. Sci. **101** (2014) 113-138.

[20] A. Mohebbi, M. Dehghan, *High order solution of one-dimensional Sine-Gordon equation using compact finite difference and DIRKN methods*, Math. Comput. Model. **51** (2010) 537-549.

[21] R. Mokhtari, M. Mohammadi, *Numerical solution of GRLW equation using Sinc-collocation method*, Comput. Phys. Comm. **81** (2010) 1266-1274.

[22] A.V. Porubov, A.L. Fradkov, B.R. Andrievsky, R.S. Bondarenkov, *Feedback control of the Sine-Gordon antikink*, Wave Motion **65** (2016) 147-155.

[23] J.I. Ramos, *The Sine-Gordon equation in the finite line*, Appl. Math. Comput. **124** (2001) 45-93.

[24] F. Saberi Zafarghandi, M. Mohammadi, *Numerical approximations for the Riesz space fractional advection-dispersion equations via radial basis functions*, Appl. Numer. Math. **144** (2019) 59-82.

[25] S.A. Sarra, Y. Bai, *A rational radial basis function method for accuratly resolving discontinuities and steep gradients*, Appl. Numer. Math. **130** (2018) 131-142.

[26] W. Shao, X. Wu, *The numerical solution of the nonlinear Klein-Gordon and Sine-Gordon equations using the Chebyshev tau meshless method*, Comput. Phys. Comm. **185** (2014) 1399-1409.

[27] A. Taleei, M. Dehghan, *A pseudo-spectral method that uses an overlapping multidomain technique for the numerical solution of Sine-Gordon equation in one and two spatial dimensions*, Math. Methods Appl. Sci. **37** (2014) 1909-1923.

[28] H. Wendland, *Scattered Data Approximation*, Cambridge University Press, 2004.